

Vorticity balance in 2-degree ECCO global ocean simulations constrained by satellite and WOCE data

Yoyu Lu and Detlef Stammer Scripps Institution of Oceanography <http://www.ecco-group.org>

Motivation

We attempt to examine the following issues from the analyses of model results:

- The role of density-topography interaction (bottom-pressure-torque) in setting the time-mean circulation;
- Evidence of Sverdrup relation in the upper ocean;
- Mid-depth circulation: geostrophic vorticity relation and zonal bands in velocity field;
- Deep flow: are model solutions consistent with Stommel-Arons theory?
- The difference between the constrained and control runs: what are the impacts of changing initial condition and surface forcing?

Model setup

• **Model** is the MITgcm and its adjoint (<http://mitgcm.org/>). Data being assimilated are satellite altimetry, Levitus monthly climatology, and surface forcing fields from NCEP/NCAR re-analysis (Stammer et al 2002). Model resolution is $2^\circ \times 2^\circ$ in longitude/latitude and 22 levels in vertical. Model simulations cover 9 years from 1992-2000. Time averaged fields from the last 7 years are analyzed and presented below. Two model runs are analyzed:

• **Control run:** initialized with T-S climatology (Levitus et al. 1994); forced by NCEP/NCAR wind, heat and virtual salt fluxes, plus restoring to SST and SSS.

• **Constrained run:** uses optimized initial T-S and surface forcing; no restoring to SST and SSS.

Depth-integrated flow

Vorticity equation

$$\beta V = \text{curl}(\tau^*) + \text{BPT} + \text{LFT} + \text{ADV} \quad (1)$$

LFT = curl of lateral friction; ADV = curl of advection of momentum; bottom-pressure-torque $\text{BPT} = \text{curl}(-\int_{\rho_0}^{\rho} \nabla p / \rho_0 dz)$, which is mathematically equivalent to $\text{BPT} = J(p/\rho_0, H)$.

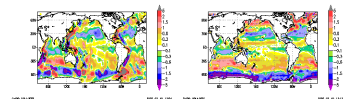


Fig. 1: The distribution of βV (left) and $\text{curl}(\tau^*)$ (right) for the depth-integrated circulation from the constrained run (in $10^{-10} \text{ m}^2 \text{ s}^{-2}$).

• **Constrained run:** On large scale direct correspondence between βV and $\text{curl}(\tau^*)$ is found in the interior of basins away from the western boundaries.

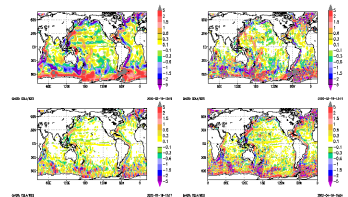


Fig. 2: The distribution of $\beta V - \text{curl}(\tau^*)$, BPT, LFT and ADV (in $10^{-10} \text{ m}^2 \text{ s}^{-2}$).

• Imbalance between βV and $\text{curl}(\tau^*)$ occurs on smaller scales near WBCs, in the subpolar North Atlantic and over the Southern Ocean, where large values of BPT, LFT and ADV are found. In interior basins the deviation of βV from $\text{curl}(\tau^*)$ is primarily balanced by BPT. The difference $\beta V - \text{curl}(\tau^*)$ shows zonally-banded structures, especially in the North Pacific, which correspond to similar features in the LFT and ADV terms.

• **Control run** shows similar distributions of the above quantities as the constrained run. Differences in magnitudes are significant. The zonal bands are contained in the original NCEP winds, but get enhanced through data assimilation.

Upper ocean (surface to 985 m)

$$\beta V = \text{curl}(\tau^*) - f w_{985} + \text{LFT} \quad (2)$$

w_{985} = vertical velocity at 985 m.

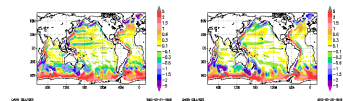


Fig. 3: The distribution of $\beta V - \text{curl}(\tau^*)$ (in $10^{-10} \text{ m}^2 \text{ s}^{-2}$) for the upper ocean from the constrained run (left) and control (right) runs.

• An approximate balance between βV and $\text{curl}(\tau^*)$ can be found in the interior of the Atlantic, Pacific and Indian Oceans. Departure from Sverdrup balance is obvious in the WBCs and at high latitudes. In the North Pacific the difference $\beta V - \text{curl}(\tau^*)$ is confined to zonal bands for both runs.

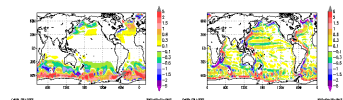


Fig. 4: The distribution of $-f w_{985}$ and $\text{LFT} + \text{ADV}$ for the upper ocean from the constrained run (in $10^{-10} \text{ m}^2 \text{ s}^{-2}$).

• At high latitudes the imbalance between βV and $\text{curl}(\tau^*)$ has a close correspondence with $-f w_{985}$. Large values of $\text{LFT} + \text{ADV}$ are found at high latitudes, near WBCs and near the equator. In the Southern Ocean $\text{LFT} + \text{ADV}$ is less important than $-f w_{985}$ in closing the vorticity budget. In WBC and at low latitudes, $\text{LFT} + \text{LFT}$ becomes more important than $-f w_{985}$.

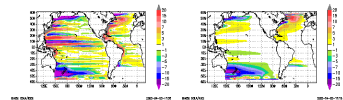


Fig. 5: Zonal integration from the eastern boundaries of Pacific and Atlantic of $V - \text{curl}(\tau^*)/\beta$ (left) and $-f w_{985}/\beta$ (right) from the constrained run (in Sv).

• The zonally-integrated $V - \text{curl}(\tau^*)/\beta$ illustrates once again that the Sverdrup relation does not hold uniformly. Over the subpolar gyre and in the western part of subtropical gyres, the departure can be explained by the zonal integral of $-f w_{985}/\beta$. In the interior subtropical areas the departure is dominated by the zonally-banded structures that are balanced by $(\text{LFT} + \text{ADV})/\beta$. Such a balance is neither geostrophic nor related to Ekman effects. The zonal bands correlate with the large lateral shear in the gyre circulation. While the lateral friction and nonlinear terms are not dominant in the moment equation, their curls become significant in the vorticity equation and do upset the geostrophic vorticity relation.

Intermediate layer (985 m to 2200 m)

$$\beta V = \int w_{985} - w_{2200} + \text{LFT} + \text{ADV} \quad (3)$$

w_{985} = vertical velocity 985 m; w_{2200} = vertical velocity 2200 m; viscous stresses at 985 m and 2200 m are neglected.

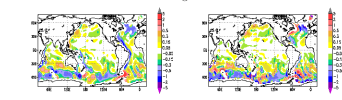


Fig. 6: The distribution of βV (left) and $f w_{985} - w_{2200}$ (right) in the intermediate layer from the constrained run (in $10^{-10} \text{ m}^2 \text{ s}^{-2}$).

• The βV term is negligible at low latitudes away from WBCs. In the interior basins βV is balanced by vortex stretching/compression. Near the WBCs, βV is mainly balanced by $\text{LFT} + \text{ADV}$.

Deep ocean (2200 m to sea floor)

$$\beta V = f w_{2200} + \text{BPT} + \text{LFT} \quad (4)$$

w_{2200} = vertical velocity at 2200 m.

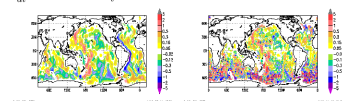


Fig. 7: The distribution of βV and $\text{BPT} + f w_{2200}$ in the deep layer from the constrained run (in $10^{-10} \text{ m}^2 \text{ s}^{-2}$).

• Away from the Southern Ocean, βV is well balanced by $f w_{2200} + \text{BPT}$. The large meridional flow near topographic features are due mostly to BPT, instead of $f w_{2200}$. In the Southern Ocean there are large cancellations between BPT and $f w_{2200}$.

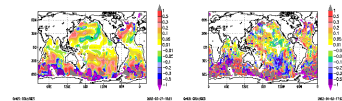


Fig. 8: Difference between the constrained and control runs in the deep layer: $\Delta(f w_{2200})$ and $\Delta(\text{BPT})$ from the constrained run (in $10^{-10} \text{ m}^2 \text{ s}^{-2}$).

• Differences $\Delta(f w_{2200})$ and $\Delta(\text{BPT})$ between the constrained and control runs are quite significant both in the interior basins and in the deep WBCs. Additional test run is conducted which is driven by the same forcing as the constrained run but initialized the same as the control run. With the exception of the Atlantic WBC the test run is much closer to the control run. Hence the change in initial density field has significant impact on abyssal flow field.

Mid-depth and deep ocean circulation

• **Mid-depth flow** is the strongest in the ACC. In N. Atlantic the broad southward flow becomes nearly zonal near 30°N , forming a narrow WBC that subsequently crosses the equator. In S. Atlantic there are two branches of near-zonal flow. In the Pacific, the intermediate flow is weak and confined to a series of zonal bands. These bands are similar to those shown by Nakano and Sugimotohara (2002) from a global ocean simulation using $1^\circ \times 1^\circ$ resolution. The zonal flows at mid-depth can be traced back to the gyre circulation in the upper ocean driven by wind, which is also mainly in the zonal direction.

• **Deep flow:** In the Atlantic the deep western boundary current flows all the way from Labrador Sea to the Southern Ocean. In the Pacific a deep current also exists near the western boundary, but flows northward. The deep circulation is strongly influenced by topography, for example, the mid-Atlantic ridge.

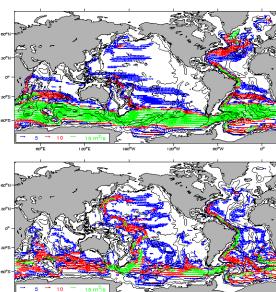


Fig. 9: Volume transport in the intermediate layer (upper) and deep layer (lower) from the constrained run. Isotherms of 2000 m, 3000 m and 4000 m are shown by black curves.

Summary

For the **depth-integrated circulation** bottom pressure torque (BPT) plays an important role in the WBCs and in the Southern Ocean. BPT usually dominates over the curl of lateral friction, especially in the Southern Ocean. For the **upper ocean** from surface to 1000 m depth, the classic Sverdrup balance holds only approximately in the interior Pacific and Atlantic Oceans. Departures from the Sverdrup relation in the interior basins are still evident, and, especially in the North Pacific, are confined to some bands in the zonal direction. These zonal bands correspond to large shear in the gyre circulation. Within these bands the curl of lateral friction is large, whereas the vortex stretching/compression due to vertical velocity is not. In the **intermediate layer**, the vortex stretching/compression associated with vertical motions drive the meridional flow in the interior basins. In the **deep ocean**, the circulation is strongly influenced by topography variations. The vertical motion at depth is complicated. At high latitudes there are large cancellations between BPT and vorticity compressing due to vertical motion. The meridional flow in the abyssal ocean is driven by the combined effect of BPT and vertical motions. The simulated abyssal circulation in the interior basins bears little resemblance with the prediction of the Stommel-Arons theory.

References

- [1] Hughes, C. W. and B. A. de Cuevas, 2001: Why western boundary currents in realistic oceans are inviscid: a link between form stress and bottom pressure torques. *J. Phys. Oceanogr.*, **31**, 2871-2885.
- [2] Lu, Y. and Stammer, 2002: Vorticity balance in coarse-resolution global ocean simulations, to be submitted.
- [3] Nakano, H. and N. Sugimotohara, 2002: A series of middepth zonal flows in the Pacific driven by winds. *J. Phys. Oceanogr.*, **32**, 161-176.
- [4] Stammer, D., C. Wunsch, R. Giering, C. Eckert, P. Heimbach, J. Marotzke, A. Adcroft, C.N. Hill and J. Marshall, 2002: The global ocean circulation during 1992-1997, estimated from ocean observations and a general circulation model. *J. Geophys. Res.*, in press.